DR. YUGUO LI (Orcid ID : 0000-0002-2281-4529)

Article type : Original Article

Original Article

Routes of transmission of influenza A H1N1, SARS CoV and norovirus in air cabin: Comparative analyses

Authors and affiliation

Hao Lei[1], Yuguo Li[1], Shenglan Xiao[1], Chao-Hsin Lin[2], Sharon L Norris[2], Daniel Wei[2], Zhongmin Hu[3], and Shengcheng Ji[3]

[1]Department of Mechanical Engineering, The University of Hong Kong, Pokfulam Road, Hong Kong SAR, China
[2]Environmental Control Systems, Boeing Commercial Airplanes, Everett, WA, USA
[3]Beijing Aeronautical Science & Technology Research Institute of COMAC, Beijing, China

Correspondence

Yuguo Li,
Department of Mechanical Engineering, The University of Hong Kong, Pokfulam Road, Hong Kong SAR, China.
Tel: (852) 3917 2625
Email: liyg@hku.hk

Routes of transmission of influenza A H1N1, SARS CoV and norovirus in air cabin: Comparative analyses

Abstract

Identifying the exact transmission route(s) of infectious diseases in indoor environments is a crucial step in developing effective intervention strategies. In this study, we proposed a comparative analysis approach and built a model to simulate outbreaks of three different inflight infections in a similar cabin environment, i.e., influenza A H1N1, severe acute respiratory syndrome (SARS) coronavirus (CoV), and norovirus. The simulation results seemed to suggest that the close contact route was probably the most significant route (contributes 70%, 95% confidence interval (CI): 67%-72%) in the inflight transmission of influenza A H1N1 transmission; as a result, passengers within two rows of the index case had

This article has been accepted for publication and undergone full peer review but has not been through the copyediting, typesetting, pagination and proofreading process, which may lead to differences between this version and the Version of Record. Please cite this article as doi: 10.1111/ina.12445

a significantly higher infection risk than others in the outbreak (relative risk (RR): 13.4, 95% CI: 1.5-121.2, *P*=0.019). For SARS CoV, the airborne, close contact and fomite routes contributed 21% (95% CI: 19%-23%), 29% (95% CI: 27%-31%), and 50% (95% CI: 48%-53%) respectively. For norovirus, the simulation results suggested that the fomite route played the dominant role (contributes 85%, 95% CI: 83%-87%) in most cases; as a result, passengers in aisle seats had a significantly higher infection risk than others (RR: 9.5, 95% CI: 1.2-77.4, *P*=0.022). This work highlighted a method for using observed outbreak data to analyze the roles of different infection transmission routes.

Keywords*: air cabin, inflight infection*, *mathematical model, multi-route transmission, outbreak, intervention*

Practical Implications

Our identification of the dominated routes, i.e. the close contact route (large droplet) for influenza, the fomite route for norovirus, and all three routes for SARS CoV suggested the relative importance of different environment intervention for different infectious diseases in air cabins and probably also in other indoor environments. For minimizing inflight fomite transmission, the aisle seatbacks and toilets should be cleaned and disinfected effectively.

1 Introduction

Knowledge about the relative importance of different transmission route(s) is fundamental to developing effective intervention strategies for infectious respiratory and enteric diseases in indoor environments. Epidemiological analysis together with in-depth environmental investigations often provides useful insights,[1] and meta-analysis may also be carried out for a particular disease. In this study, we proposed an alternative comparative analysis approach in which we studied outbreaks of different diseases in the same environment using the same approach, by examining differences in the spatial infection patterns. This approach could partly overcome the limitation of traditional individual outbreak analysis that outbreak can't be repeatedly observed, because the comparative analysis of different diseases in the same environment is like that one disease happened several times. Our hypothesis is that the different transmission routes of infection lead to different spatial patterns of secondary cases. For example, close contact transmission always happens with 1 to 2 meters of the source, which means that secondary cases infected via close contact route would be close to the index case(s). The airborne transmission may occur over long distance, and the secondary cases infected via airborne route would distribute uniformly in a space when the air is fully mixed.

Aircraft cabins were selected as the context for our study. The more or less fixed seating arrangement in aircraft cabins permits a spatial pattern of the secondary cases to be identified in some outbreaks. The temporal and spatial variation of the environment in aircraft cabins is also not as great as it is in other environmental spaces. Understanding transmission routes in

aircraft cabins is itself an important issue for not only onboard intervention, but also the worldwide infection transmission since air travel had been proved to be important in the 2003 severe acute respiratory syndrome (SARS) outbreak and 2009 influenza A H1N1 outbreak.[2] Confined space, limited ventilation, re-circulated air and/or prolonged exposure times, which are common in air travel, are demonstrated risk factors for the transmission of infectious diseases,[3] such as tuberculosis, influenza, common cold, SARS and gastroenteritis.

Our study focused on three viruses: influenza A H1N1, SARS coronavirus (CoV), and norovirus. The 1918 influenza pandemic killed 20-40 million people, and influenza can still kill thousands each year.[4] SARS CoV outbreaks in 2003 caused thousands of deaths around the world. Norovirus is the leading cause of nonbacterial gastroenteritis in human.[5,6] The three major possible routes in aircraft cabins are close contact, airborne, and fomite.[7]

In this study, a mathematical model was built to study the inflight infection transmission process, based on the studies by Atkinson and Wein[8] and Nicas and Jones.[9] This technique enables detailed physical and biological processes to be modeled, and the impact of environmental parameters to be easily integrated. We compared the simulated relative importance of different transmission routes in three inflight outbreaks with the reported spatial distribution of the secondary cases.

2 Data and Methods

2.1 Three chosen outbreaks

We performed a literature search for inflight outbreaks of influenza A H1N1, SARS CoV, and norovirus in Supplementary A. All three chosen outbreaks occurred in Boeing 737 aircraft cabins with flight duration 2.5 or 3 hours. The main criteria for identifying suitable outbreaks include the availability of detailed seating information for both the infected and non-infected, airplane type and flight duration. Figure 1 illustrates the detailed spatial distribution of the secondary cases in the chosen outbreaks.

2.2 Multi-route disease transmission model

The definitions for the relevant transmission routes (Figure 2) in our multi-route model are as follows.

The airborne route refers to direct inhalation of an infectious agent through small droplet nuclei, i.e., the residue of large droplets containing microorganisms that have evaporated to an aerodynamic diameter of less than 10 microns (termed respirable).[9] These respirable droplets can deposit in the respiratory tract.

Close contact route includes direct contact and large droplet transmission. Direct contact refers to infection through person-to-person contact with the index source passenger, such as hand-shaking. We assume there is no body-to-body contact between index source passenger(s) and other passengers during the flight. We only consider large droplet transmission in the model, which refers to the *inhalation* of the virus carried in respirable airborne particles with a diameter between 10 and 100 microns (termed inspirable),[9] and the *droplet spray* of large droplets (>100 microns in diameter) onto facial target membranes.

The fomite route refers to infection by touching objects or surfaces that have earlier been contaminated by hands or by direct deposition of infectious pathogens from the index source passenger, which is also sometimes termed indirect contact route.

Virus-containing droplets generation

For **respiratory disease**, coughing is used as surrogate to model the virus-containing droplets from all respiratory activities such as breathing, talking, and sneezing, as the size distribution of the droplets from coughing, talking and sneezing is similar, and the amount of droplets generated due to breathing is negligible. Assume that cough frequency for infector is f_c per hour and that one cough can produce N_c droplets with the size distribution $F_c(r_0)$. Then the generation rate (number/h) of droplets with radius r_0 (μm) from individual i, $G_i(r_0) = f_c N_c F_c(r_0)$.

For **enteric disease**, such as norovirus, virus-containing droplets are emitted from the infector in vomit and/or diarrhea. A study by simulated vomiting device showed that the volume of the aerosolized droplets ranged from 0.004 mL to 21 mL, with a mean value of 0.4 mL.[10] To the best of our knowledge, there is no study on the size distribution of the droplets from vomit, we assume that these droplets have same size distribution as those from coughing.

Fates and concentration of virus-containing droplets in air cabin

For **respirable droplets** with aerodynamic diameter of less than 10 microns, they could move a long distance with the air flow and distribute in the air in cabin with volume V (m^3). Liu et al. studied respirable droplets concentration at different distance away from the source and found that respirable droplet concentration is uniform everywhere except within 1 m of the source.[11] A concentration ratio $\varepsilon_c(s_i) = C_l^i(r,t)/C_e(r,t)$ was defined, where $C_l^i(r,t)$ was the number concentration (number/m^3) of the airborne droplets in the inhaled air of individual i with radius r at time t; $C_e(r,t)$ was the droplet nuclei concentration (number/m^3) out of 1 meter of the index case. A simple model adapted from Liu et al.[11] was used to describe the concentration ratio at distance s (m) away from the source, in Equation (1):

$$\varepsilon_c(s) = \begin{cases} -6s + 7, s < 1 \\ 1, s \geq 1 \end{cases} \quad (1)$$

For **inspirable droplets** with a diameter between 10 and 100 microns, we assumed that the maximum horizontal distance they could move was 2 m because of gravity and the relatively high deposition rate on environmental surfaces. They distributed within two meters of the source, and the volume of this space was denoted to be V_2 (m^3).

A rapid death rate of pathogens atomized into air had been observed[12,13] and evaporation of droplets was believed to play an important role.[14] Xie et al.[15] found that there was a fast viability decline stage when the droplets completely evaporated, when viability decreased to about 25% and then slowly declined. Here, the survival ratio due to evaporation was defined as $\varepsilon_e(r_0, s) = L(r_0, t)/L(r_0, 0)$

$$\varepsilon_e(r_0, s) = \begin{cases} 1, & if\ T_e(r_0) > T_m(s) \\ 0.25, & if\ T_e(r_0) < T_m(s) \end{cases} \quad (2)$$

where $L(r_0, t)$ is the concentration of viable viruses ($TCID_{50}$/ml or genome copies/ml) in droplets with initial radius r_0 (μm) at the time t (s) after being exhaled; $T_e(r_0)$ is the evaporation time (s) for the droplets with radius r_0 (μm); $T_m(s)$ is the travelling time (s) for the exhaled droplets from the source to reach a susceptible individual a distance s (m) away. Xie et al.[16] studied the evaporation time of droplets with different diameters, and a fitting function $T_e(r_0) = \beta_e {r_0}^2$ was used in this study, where $\beta_e = 7 \times 10^{-4}$ s/μm^2. $T_m(s) = s/V_m$, where V_m is droplet speed (m/s) and s is the distance (m) away from the index case. The advective flow velocity toward the cabin aft is about 0.1m/s.[17] And according to one field experiment in the first class cabin, 72% of the test points in the cabin had a velocity lower than 0.1m/s, so in this study, we assume that the average airflow velocity in the air cabin is 0.1 m/s and V_m is also 0.1m/s.[18]

Assume there is no resuspension of droplets from environmental surfaces into the air. In the air cabin, on one hand, viable virus is generated from index case(s) at rate $\sum_{i=1}^{N} I_i G_i(r_0) L(r_0, 0)$, where I_i is the index of individual i (if individual i is the infector, $I_i = 1$, else $I_i = 0$); The contribution of viable viruses from the 50% return air is ignored as the HEPA filter efficiency is very high, and the minimum efficiency can be as high as 99.97%. [19] On the other hand, the viable viable virus-containing droplets are removed from the cabin by ventilation system at rate q and q=25/h,[20] natural inactivation at rate b_a (/h); deposition on environmental surfaces at rate $k_d r^2$ (/h).

For **respirable droplets**, which are distributed in the air cabin with volume V (m^3), we have

$$\frac{d\left(\int_0^V \varepsilon_c(s) C_e(r_0) L(r_0, t) dv\right)}{dt} = \sum_{i=1}^{N} I_i G_i(r_0) L(r_0, 0) - (q + b_a + k_d r^2) V\, C_e(r, t) L(r_0, t) \quad (3)$$

For **inspirable droplets**, which are distributed in the space of volume V_2 (m^3) within two meters of the index case, similarly, we have

$$d(\int_0^{V_2} \varepsilon_c(s) C_b(r_0) L(r_0,t) dv)/dt = G_i(r_0) L(r_0,0) - (q + b_a + k_d r^2) V_2 C_b(r,t) L(r_0,t) \quad (4)$$

where $C_b(r)$ is the droplets concentration (number/m^3) at the boundary of the space within 2 meters of the index case.

For **influenza and SARS**, viable virus-containing droplets are emitted continuously through coughing, we assumed that the concentration of the virus-containing droplets would reach a steady state, then we have

$$C_e(r,t) L(r_0,t) = \sum_{i=1}^{N} I_i G_i(r_0) L(r_0,0) \ /((q + b_a + k_d r^2) V) \quad (5)$$

And

$$C_b(r,t) L(r_0,t) = G_i(r_0) L(r_0,0)/((q + b_a + k_d r^2) V_2) \quad (6)$$

For **norovirus**, virus-containing droplets are emitted from the infector in vomit and/or diarrhea, which are rarer than coughs, so in the norovirus outbreak it is not reasonable to assume that the airborne virus-containing droplet concentration from vomit or diarrrhea will achieve a steady state. After each vomiting or diarrheal episode, we therefore assumed the droplets would quickly and uniformly distribute in the air, which was set as the initial condition. The concentration of the viabble norovirus-containing airborne droplets ($C_n(r,t)$, number/m^3) in the air cabin could be calculated according to the following equation:

$$V \frac{\mathrm{d}(C_n(r,t) L(r_0,t))}{\mathrm{dt}} = -(q + b_a + k_d r^2) V C_n(r,t) L(r_0,t)$$

$$C_n(r,t_0) = N_v Pr F_c(r_0)/V, \text{ for } r < 5\ \mu\text{m} \quad (7)$$

where t_0 is the time when the vomit or diarrhea accident occurs; N_v is the number of aerosolized droplets generated during each vomit; Pr is the assumed percentage of respirable droplets emitted into the air, so if patient(s) vomit on the ground, $Pr = 1$, and if they vomit into sickbags, $Pr = 0.1$. Predicted results with different percentages of airborne droplets emitted from sickbags are compared in Supplementary C. The solution of Equation (7) was

$$C_n(r,t) L(r_0,t) = C_n(r,t_0) e^{-(q+b_a+k_d r^2)(t-t_0)} \quad (8)$$

The exposure through each route was modeled separately, and then the dose response model was used to assess an integrated risk.

Exposure via airborne route

The dose to individual i via the airborne route in the lower and upper respiratory tract are denoted as D_{al}^{i} and D_{au}^{i} ($TCID_{50}$ or genome copies), and for a flight duration T, they can estimated as follows:

$$D_{al}^{i} = \int_{o}^{T} \int_{0}^{r_a} C_l^i(r,t) p \delta_l(r) t \frac{4}{3} \pi r_0^3 L(r_0,t) dr\, dt$$

$$D_{au}^{i} = \int_{o}^{T} \int_{0}^{r_a} C_l^i(r,t) p \delta_u(r) t \frac{4}{3} \pi r_0^3 L(r_0,t) dr\, dt \quad (9)$$

where r_a is the largest radius for airborne droplets and $r_a = 5$ μm;[9] p is the pulmonary ventilation rate and $p = 0.48$ m^3/h;[21] r_0 is the droplets' initial radius and r is the final radius after complete evaporation. Here we assume that $r = r_0/3$;[10] $\delta_l(r)$ and $\delta_u(r)$ are the deposition fraction of droplets with radius r in the lower and upper respiratory tract respectively. The model from ICRP was used in this study.[22]

Exposure via close contact route

Transmission by close contact refers to either inhalation of the virus carried in airborne particles with a diameter between 10 and 100 microns, or the spray of large droplets on the susceptible individuals' mucous membranes.

For norovirus transmission, it is difficult for the "large" droplets generated from vomiting to move to the inhale air of the seated susceptible passengers, which is always more than one meter above the ground, because of the high downward velocity, gravity and the relatively high deposition rate. Therefore, the close contact route was not considered in the norovirus transmission.

Then the dose via inhalation of inspirable droplets in upper respiratory tract (D_{cr}^{i} ($TCID_{50}$ or genome copies)) was

$$D_{cr}^{i} = \int_{o}^{T} \int_{r_a}^{r_b} \varepsilon_c(s_i) C_b(r,t) pt\ \delta_u(r) \frac{4}{3} \pi r_0^3 L(r_0,t) dr\, dt \quad (10)$$

where r_b was radius of the maximum inspirable droplets and $r_b = 50$ μm.[9]

For the spray of large droplets on mucous membranes, because of the seating arrangement we assumed that there was no face-to-face droplet spray on susceptible individual mucous membranes. In this study a simple model was used, in which it was assumed that the number of droplets deposited on one surface was proportional to its area. Denote the total surface area of the space within two meters of the index case as A_{V_2} (m^2) and the area of mucous membrane of one person as A_m (m^2). In the space within 2 meters of the index case, there are 30 seats (5 rows and 6 seats per row) with area 1 m^2 for each, and the human body surface area is about 1.75 m^2, and there are overlaps between body and seat surfaces when sitting, so an estimated area 2 m^2 is used for each seat and the passengers sitting on it. The floor area is $4\text{m} \times 3.2\text{m} = 12.8\ m^2$, so an estimated value for $A_{V_2} = 30 \times 2\ m^2 + 12.8\ m^2 = 72.8\ m^2$,

and $A_m = 0.001\ \mathrm{m}^2$ is used in this study. The dose via the close contact route due to deposition on mucous membrane is

$$D_{cm}^{i} = \int_{o}^{T} \int_{r_a}^{\infty} \frac{A_m}{A_{V_2}} C_c^i(r) k r^2 V_2 t \frac{4}{3} \pi r_0^3 L(r_0, t) dr\, dt \tag{11}$$

Exposure via fomite route

A Markov Chain was built to model the fomite route infection transmission. Define a matrix $Ps = (ps(k))_{N_s \times N_p}$, which shows surface-touching behaviour. If on time step k, individual i touched surface j, $ps_{j,i}(k)$=1, else $ps_{j,i}(k) = 0$. Denote the virus concentration on individual i hand and environmental surface j at time k by $C_h^i(k)$ and $C_s^j(k)$ (TCID_{50} or genome copies/m^2) respectively. In the next time step $k+1$ after time ΔT, the number of infectious pathogens on the hand contact area on the environmental surfaces j is

$$C_s^j(k+1) = (C_s^j(k) + \frac{\sum_{i=1}^{N_p} (C_h^i(k) A_{hs} \tau_{hs} - C_s^j(k) A_{hs} \tau_{sh}) ps_{i,j}(k)}{A_s}) e^{-b_s \times \Delta T} \tag{12}$$

where A_{hs} is the connection area (m^2) between hand and the environmental surface during contact, A_s is the area (m^2) of surface j. We estimated $A_{hs} = 0.0042\ \mathrm{m}^2$;[23] τ_{hs} is the pathogen transfer efficiency from hand to environmental surface; τ_{sh} is the pathogen transfer efficiency from surface to hand; b_s is the first-order (exponential) inactivation rate (/h) of pathogens on environmental surfaces.

Denote $pm_i(k)$ as the mucous membranes touching behaviour of individual i, i.e. if at time interval k, individual i touches his/her mucous membranes, $pm_i(k) = 1$, else $pm_i(k) = 0$. It is assumed that a touch on the mucous membranes involves only one fingertip of the same hand that touches the contaminated environmental surfaces, and this process is a one-way transmission, i.e. from hand to mucous membranes.

Then the virus concentration on individual i hand at time $k+1$ is

$$C_h^i(k+1) = (C_h^i(k) - \frac{\sum_{i=1}^{N_p} (C_h^i(k) A_{hs} \tau_{hs} - C_s^j(k) A_{hs} \tau_{sh}) ps_{i,j}(k)}{A_h} - \frac{pm_i(k) A_h^m \tau_{hm} C_h^i(k)}{A_h}) e^{-b_h \times \Delta T} \tag{13}$$

where A_h is the hand palm area (m^2), which was estimated to be $0.0203\ \mathrm{m}^2$;[24] b_h is the pathogens' first-order inactivation rate (/h) on hands; τ_{hm} is the virus transmission efficiency from hand to mucous membranes; A_h^m is the hand-to-mucous membrane connection area (m^2), and A_h^m is assumed to be $0.0001\ \mathrm{m}^2$.

Given the initial condition ($k = 0$) of the virus concentration on all of the environmental surfaces, then the virus concentration in each time interval can be calculated. The total dose to individual i via the fomite route is

$$D_{fm}^{i} = \sum_{k=1}^{N_t} Pm_i(k) A_h^m \tau_{hm} C_h^i(k) \quad (14)$$

where N_t is the total time intervals and $N_t = \left\lfloor \frac{T}{\Delta T} \right\rfloor$, T is the flight duration and $\lfloor\ \rfloor$ is the floor function.

Infection risk assessment

The negative exponential dose response model was used to estimate the infection risk, which implies that a single particle can start an infection, all single particles are independent of each other. The infection risk of individual i during the flight can be calculated according to the following equation

$$P_i = 1 - e^{[-(\eta_l D_{al}^i + \eta_u D_{au}^i) - (\eta_u D_{cr}^i + \eta_m D_{cm}^i) - \eta_m D_{fm}^i]} \quad (15)$$

where η_l, η_u and η_m are the dose response rates (/$TCID_{50}$ or /genome copy) in lower/upper respiratory tracts, and on mucous membranes respectively. Here it's also assumed that $\eta_u = \eta_m$.

2.3 Model Parameterization

Many parameters in the model are uncertain. For example, different viruses may have different infectivity, survivability and shedding profiles. Even for the same virus, different populations may have different susceptibility. We use value from empirical literatures as well as our estimation for these parameters, and we also apply lower and upper parameter constraints for 7 categories of parameters that have been proved to be significantly correlated with the model reproductive number (see detail in Supplementary B).[25] The probability distribution of each parameter in these seven categories is defined as follow: uniformly distributed from lower constraint to median value, and from median value to upper constraint, in addition, the mean value of the distribution is equal to the median value. As there was some randomness in the choice of the parameter values, for each case, the simulation was implemented with 400 replications, which are sufficient to generate statistical stability, since the difference between the simulated percentage contribution of each route with 400 replications and 800 replications was less than 3% (see detail in Supplementary D).

Due to the large range of the virus shedding magnitude, there was a large range in the simulated number of infected passengers during flight in these 400 replications. In addition, during the 2.5- 3-hour flight, the virus shedding magnitude was relatively stable for each index case, as the virus concentration in the exhaled droplets was relatively stable during such a short period. Therefore, to quantitatively compare with the reported outbreak data, we narrowed the shedding magnitude value in each outbreak so that the simulated mean infection risk for all of the passengers in these 400 replications was close to the reported attack rate. In the influenza outbreak simulation, the virus shedding magnitude was set to between 1.8×10^{12} and 1.8×10^{13} $TCID_{50}$/(mL·h) (the constraints for this parameter ranged from 1.8×10^{9} to 1.8×10^{13}); in the SARS CoV outbreak, the virus shedding magnitude was set to between 1.8×10^{12} and 1.8×10^{13} mRNA copies/(mL·h) (the constraints for this parameter ranged from

1.8×10^{9} to 1.8×10^{13}); in the norovirus outbreak, the virus shedding magnitude was set to between 2×10^{14} and 2×10^{15} genome copies/(mL·h) (the constraints for this parameter is from 3×10^{13} to 3×10^{17}).

3 Results

Figure 3 provides the distribution of infected passengers and percentage contribution for each route in three outbreaks during these 400 replications, with the full range of the virus shedding magnitudes. In the influenza A H1N1 inflight transmission, in most cases, the number of passengers infected via the fomite route was much less than the number infected via the airborne and close contact routes, and more were infected via the close contact route than via the airborne route. In the SARS CoV inflight transmission, the numbers of passengers infected via all three routes had a similar order of magnitude. In the inflight norovirus outbreak, the close contact route was not considered, and in most cases, the number of passengers infected via the fomite route was much higher than the number infected via the airborne route.

Table 1 summarizes the attack rate from reported outbreak data, and the predicted average infection risk and simulated number passenger infected (mean and 95% confidence interval (CI) of 400 replications) via three routes respectively in the three outbreaks with the tuned range of virus shedding magnitudes. Here, the attack rate is defined as the number of infected divided by the number of interviewed susceptible individuals. Under the chosen range of virus shedding magnitude, the simulated infection risks fit well with the reported attack rates in three outbreaks. Under this situation, the close contact route is suggested to contribute most in the inflight influenza A H1N1 transmission (contributes 70%, 95% CI: 67%-72%, of the transmission, contribution of one route is defined as the number passenger infected via this route divided by the total number passenger infected via three routes together). In inflight SARS CoV transmission, airborne, close contact and fomite route contribute 21% (95% CI: 19%-23%), 29% (95% CI: 27%-31%), and 50% (95% CI: 48%-53%) respectively. The fomite route plays the dominant role (contributes 85%, 95% CI: 83%-87%) in the inflight norovirus transmission.

Different routes are expected to lead to different spatial distributions of secondary cases. For example, the close contact route causes a much higher infection risk for those sitting close to the ill passengers than those seated far away. The 2009 WHO guidance suggests contact tracing passengers seated within two rows of an infectious case of influenza during air travel.[29]

Table 2 lists the infection risk for passengers seated within two rows of the ill passenger(s) and for those seated farther away from both reported data and simulation results (mean and 95% CI of 400 replications with the narrowed virus shedding magnitude). Both the predicted infection risk and reported outbreak data show that in the influenza A H1N1 inflight outbreak, the infection risk for passengers sitting within two rows of the index case is

statistically significantly higher than others, which coincides with our result that close contact route may be the most significant in the inflight influenza A H1N1 transmission.

For the fomite route, Figure 4 provides a typical seatback surface contamination network in a Boeing 737-300 air cabin environment in one simulation. The surface contamination network in air cabin has a community structure. Different communities are connected by aisle seatback surfaces and toilets, because on the way to the toilet and back to their seats, the passenger may touch some aisle seatback surfaces. The aisle seat passengers are therefore more likely to have higher dose than non-aisle through the fomite route. Table 3 compares the infection risk for the aisle and non-aisle seats from both the reported data and simulation results (mean and 95% CI of 400 replications with the narrowed virus shedding magnitude). According to the simulation results, the fomite route is suggested to play the dominant role in the norovirus inflight transmission in most cases. The report outbreak data also show that the aisle seat passengers have a significantly higher infection risk than others.

4 Discussion

In this study, we built a mathematical model to study the in-flight transmission of different viruses, using a novel comparative analysis approach. The results suggested that the dominant transmission routes in air cabins are probably the close contact route for influenza, the fomite route for norovirus, and all three routes (airborne, close contact and fomite routes) for SARS CoV. The dominant transmission routes vary for the three viruses, mainly depending on the pathogen-specific parameters, such as the inactivation rate on human hands and environmental surfaces, the virus dose response rate, and the virus concentration. The outbreak data also affirmed our main hypothesis that the different transmission routes of infection led to different spatial patterns of secondary cases, so passengers within two rows of the index case in the influenza A H1N1 outbreak and passengers in aisle seats in the inflight norovirus outbreak had a significantly higher infection risk than others.

Our results should be interpreted at least with the following caveats. Firstly, many major assumptions were made for the model parameters, and some are judgement-based and not well supported by evidence or data. For example, the SARS CoV dose response rate obtained in the mice experiments was applied to humans. In addition, the surface touching behavior, which is necessary when building a surface contamination network, is expected to vary very significantly, but we assumed that the same behavior is applied uniformly both in time and for individuals during the entire flight. The surface contamination network may be improved as more behavior data become available. Furthermore, the distribution and the constraints for each parameter set that were used might also not be realistic. These assumptions may challenge the conclusion that the fomite route is the dominant one for norovirus. Secondly, only one outbreak was available for our analysis for each virus. Generalization of findings due to one outbreak is questionable. Lastly, we have not considered the possibility of infection before and after the flight, such as during check-in and in the lounge, which suggests that our analysis might have overestimated the overall inflight risk.

Our comparative analysis approach for multiple outbreaks and viruses differs from the traditional individual analysis of an outbreak.[1] The same mechanisms of fomites (e.g., surface or object contamination network) and bio-aerosol transport (i.e., close contact and airborne) are applied to all three pathogens in the cabin, with the only differences in the pathogen-specific parameters (inactivation rate, surface transfer efficiency, etc.). In addition to previous theoretical work on relative importance of different transmission routes of influenza by Atkinson and Wein,[8] Nicas and Jones,[9] and Spicknall et al.,[25] we simulated the real outbreaks and compare the simulation results with the outbreak data.

For influenza A H1N1, due to the high inactivation rate on environmental surfaces and hands, in most cases, the total infection risk via fomite route is much lower than that via airborne route and close contact route, this is consistent with the study by Atkinson and Wein[8] in a household environment. The study by Teunis et al.[30] indicated that the infection probability of the droplet route (i.e., close contact) and the aerosol route (i.e., the airborne route) in a poorly ventilated room is approximately equal. But due to the high ventilation rate (25 per hour) and HEPA filter efficiency of ventilation system in the aircraft, and the close contact route is shown to be probably the most significant in inflight influenza transmission, so the infection risk for passengers sitting close to the index case(s) is significantly high than others. In addition, a review study on human influenza transmission of Brankston et al.[31] concluded that transmission of influenza occurs at close range rather than over a long distance. Of the five inflight influenza A H1N1 outbreaks reviewed, with detailed distribution of the secondary cases included, four showed that the passenger sitting within the first two rows of the ill passenger(s) had a higher infection risk than others. The 2009 WHO guidance recommends the contact tracing of passengers seated within two rows of an infectious case of influenza during air travel.[29] The air change rate and efficiency of the HEPA filter are relatively high in the aircraft ventilation system than other typical indoor environments, so that the airborne pathogens can be removed effectively. In most reported inflight influenza A H1N1 outbreaks, the attack rate is low (1-5%), but in the seasonal influenza A outbreak in March 1977, when the air conditioning system of a commercial airliner was shut down due to a malfunctioning engine, the attack rate reached 72%.[33]

Compared with the influenza A H1N1 virus, the SARS CoV has a much lower inactivation rate on environmental surfaces and skin, which is probably why the fomite route is more important in SARS CoV transmission than that in influenza A H1N1 transmission. Our finding supports the combined findings of airborne transmission,[1,34] large droplet transmission,[35] and fomite transmission for SARS CoV. [36] As far as we are aware there are no data on the dose response rate of SARS CoV either on mucous membranes or in the respiratory tracts of humans. We assume that the dose response rate on human mucous membranes is the same as that on mice mucous membranes, and the dose response rate in the human respiratory tract is 1000 times that of mucous membranes (similar to the influenza A H1N1 data). We also performed the sensitivity analysis of the dose response rates, with different ratios of median dose response rate, i.e. (in lower respiratory tract)/(on mucous membranes) (see detail in Supplementary E), and we found that all three routes were important in inflight SARS CoV transmission for different ratios of median dose response

rate.

The fecal-oral spread is known to be the primary mode of transmission of norovirus. [5] The fomite route transmission of norovirus is well supported by the reported widespread environmental contamination with norovirus.[37,38] Our simulation of a norovirus outbreak confirms that the fomite route is dominant in transmission. It is also suggested that vomiting can produce aerosol droplets containing norovirus particles, and inhaled by exposed susceptible individuals, depositing in the upper respiratory tract and subsequentially swallowed along with the respiratory mucus.[39] Airborne norovirus was detected from an air sample in one outbreak.[40] A study of a norovirus outbreak in a hotel found an inverse relationship between the infection risk and the distance from the person who vomited when a food source was not implicated.[41] This study simulated both the airborne and fomite route transmission of norovirus. And the results showed that in most cases, the fomite route plays the dominant role. The predicted infection risk from the fomite route for aisle seat passengers is 2.2 times higher than that for non-aisle seat passengers. The aisle passengers to non-aisle passengers relative risk in the outbreak (9.5) is much higher than 2.2, may be attributable to a small sample size of secondary cases (6).

5 Conclusions

In conclusion, a mathematical model was built to simulate the physical process of inflight transmission of influenza A H1N1, SARS CoV coronavirus, and norovirus. Our model used the same mechanisms of fomites (a surface contamination network) and bio-aerosol transport (i.e., close contact and airborne) for all pathogens in similar environment settings (air cabins), with the only differences being in the pathogen-specific parameters (e.g., inactivation rate, surface transfer efficiency). Our simulation results have some aspects that are similar to the outbreak data in terms of the spatial distribution of secondary cases. Though with uncertainties, the simulation results suggested that for inflight influenza A H1N1 transmission, the airborne and close contact routes may be much more important than the fomite route; for SARS CoV, although the fomite route is slightly more important than the other routes, it is not dominant and all three transmission routes are found to be important; for norovirus transmission, the fomite route may be dominant. Our results reveal that environment control in indoor environments should consider all three possible transmission routes for respiratory and enteric infections. Additionally, this study highlights a way to use observation outbreak data to analyze the relative importance of different routes in infection transmission.

Acknowledgements

This work was mainly funded by the Boeing Company and the Commercial Aircraft Corporation of China Ltd. This work was also supported financially by a RGC GRF project (No 17211615) of the Hong Kong SAR Government.

References

1. Yu ITS, Li YG, Wong TW, Chan TW, Tam W, Chan AT, JHW Lee, DYC Leung, Ho T. Evidence of airborne transmission of the severe acute respiratory syndrome virus. *N Engl J Med.* 2004; 350(17):1731-1739.
2. Khan K, Arino J, Hu W, et al. Spread of a novel influenza A(H1N1) virus via global airline transportation. *N Engl J Med.* 2009; 361(2): 212-214.
3. Leder K, Newman D. Respiratory infections during air travel. *Intern Med J*. 2005;35 (1):50-55.
4. Mills CE, Robins JM, Lipsitch M. Transmissibility of 1918 pandemic influenza. *Nature.* 2004;432(7019):904-906.
5. Glass RI, Parashar UD, Estes MK. Norovirus gastroenteritis. *N Engl J Med.* 2009;361(18):1776-1785.
6. Lindesmith L, Moe C, Marionneau S, Ruvoen N, Jiang X, Lindblad L, Stewart P, LePendu J, Baric R. Human susceptibility and resistance to Norwalk virus infection. *Nat Med*. 2003;9(5):548-553.
7. Mangili A, Gendreau MA. Transmission of infectious diseases during commercial air travel. *Lancet.* 2005;365(9463):989-996.
8. Atkinson MP, Wein LM. Quantifying the routes of transmission for pandemic influenza. *Bull Math Biol*. 2008;70 (3):820-867.
9. Nicas M, Jones RM. Relative contributions of four exposure pathways to influenza infection risk. *Risk Anal*. 2009;29(9):1292-1303.
10. Tung-Thompson G, Libera DA, Koch KL, Francis III L, Jaykus LA. Aerosolization of a human norovirus surrogate, bacteriophage MS2, during simulated vomiting. *Plos One*. 2015; 10(8):e0134277.
11. Liu L, Li Y, Nielsen PV, Wei J, Jensen RL. Short-range airborne transmission of expiratory droplets between two people. *Indoor Air*. 2017;27(2):452-462.
12. Cox CS. Aerosol survival of Pasteurella tularensis disseminated from the wet and dry states. *Appl Microbiol*. 1971;21(3):482-486.
13. Ehresmann DW, Hatch MT. Effect of relative humidity on the survival of airborne unicellular algae. *Appl Microbiol*. 1975;29(3):352-357.
14. Riley RL, O'Grady F. *Airborne infection: transmission and control*. New York: The Macmillan Company; 1961.
15. Xie X, Li YG, Zhang T, Fang HH. 2006. Bacterial survival in evaporating deposited droplets on a teflon-coated surface. *Appl Microbiol Biotechnol*. 2006;73 (3):703-712.
16. Xie X, Li YG, Chwang ATY, Ho PL, Seto WH. How far droplets can move in indoor environments - revisiting the Wells evaporation-falling curve. *Indoor Air*. 2007;17(3):211-225.
17. Eklund TI. Inflight cabin smoke control. *Toxicology.* 1996;115:135-144.
18. Liu W, Wen JZ, Chao JY, Yin WY, Shen C, Lai DY, Lin CH, Liu JJ, Sun HJ, Chen QY. Accurate and high-resolution boundary conditions and flow fields in the first-class cabin of an MD-82 commercial airliner. *Atmos Environ.* 2012;56:33-44.
19. Lindgren T, Norback D (2002) Cabin air quality: indoor pollutants and climate during

intercontinental flights with and without tobacco smoking. *Indoor Air.* 12 (4):263-272.
20. Jones RM, Masago Y, Bartrand T, Haas CN, Nicas M, Rose JB. Characterizing the risk of infection from Mycobacterium tuberculosis in commercial passenger aircraft using quantitative microbial risk assessment. *Risk Anal.* 2009;29 (3):355-365.
21. Chen SC, Chang CF, Liao CM. Predictive models of control strategies involved in containing indoor airborne infections. *Indoor Air.* 2006;16:469-481.
22. International Commission Radiological Protection. Human respiratory tract model for radiological protection. A report of a Task Group of the International Commission on Radiological Protection. *Ann ICRP*. 1994;24(1-3):1-482.
23. AuYeung W, Canales RA, Leckie JO. The fraction of total hand surface area involved in young children's outdoor hand-to-object contacts. *Environ Research.* 2008;108(3):294-299.
24. Lee JY, Choi JW, Kim H. Determination of hand surface area by sex and body shape using alginate. *J Physiol Anthropol.* 2007;26(4):475-483.
25. Spicknall IH, Koopman JS, Nicas M, Pujol JM, Li S, Eisenberg JNS. Informing optimal environmental influenza interventions: how the host, agent, and environment alter dominant routes of transmission. *PLoS Comput Biol*. 2010;6(10): e1000969.
26. Kirking HL, Cortes J, Burrer S, Hall AJ, Cohen NJ, Lipman H, Kim C, Daly ER, Fishbein DB. Likely transmission of norovirus on an airplane, October 2008. *Clin Infect Dis*. 2010; 50(9):1216-1221.
27. Olsen SJ, Chang HL, Cheung TYY, Tang AFY, Fisk TL, Ooi SPL, Kuo HW, Jiang DDS, Chen KT, Lando J, Hsu KH, Chen TJ, Dowell SF. Transmission of the severe acute respiratory syndrome on aircraft. *N Engl J Med*. 2003;349(25):2416-2422.
28. Neatherlin J, Cramer EH, Dubray C, Marienau KJ, Russell M, Sun H, Whaley M, Hancock K, Duong KK, Kirling HL, Schembri C, Katz JM, Cohen NJ, Fishbein DB. Influenza A(H1N1)pdm09 during air travel. *Travel Med Infect Dis*. 2013;11(2):110-118.
29. Word Heath Organization (WHO). WHO technical advice for case management of influenza A(H1N1) in air transport. 2009. *Geneva: The Organization*.
30. Teunis PFM, Brienen N, Kretzschmar MEE. High infectivity and pathogenicity of influenza A virus via aerosol and droplet transmission. *Epidemics.* 2010;2(4):215-222.
31. Brankston G, Gitterman L, Hirji Z, Lemieux C, Gardam M. Transmission of influenza A in human beings. *Lancet Infect Dis*. 2007;7:257-265.
32. Mackintosh CA, Hoffman PN. An extended model for transfer of micro-organisms via the hands: differences between organisms and the effect of alcohol disinfection. *J Hyg. (Lond)* 1984;92(3):345-355.
33. Moser MR, Bender TR, Margolis HS, Noble GR, Kendal AP, Ritter DG. An outbreak of influenza aboard a commercial airliner. *Am J Epidemiol.* 1979;110(1):1-6.
34. Li YG, Huang X, Yu ITS, Wong TW, Qian H. Role of air distribution in SARS transmission during the largest nosocomial outbreak in Hong Kong. *Indoor Air*. 2005;5(2):83-95.
35. Sze To GN, Wan MP, Chao CYH, Fang L, Melikov A. Experimental study of dispersion and deposition of expiratory aerosols in aircraft cabins and impact on infectious disease transmission. *Aerosol Sci Technol*. 2009;43(5):466-485.
36. Dowell SF, Simmerman JM, Erdman DD, Wu JSJ, Chaovavanich A, Javadi M, Yang

JY, Anderson LJ, Tong S, Ho MS. Severe acute respiratory syndrome coronavirus on hospital surfaces. *Clin Infect Dis*. 2004;39:652-657.

37. Cheesbrough JS, Green J, Gallimore CI, Wright PA, Brown DW. Widespread environmental contamination with Norwalk-like viruses (NLV) detected in a prolonged hotel outbreak of gastroenteritis. *Epidemiol Infect*. 2000;125(1):93-98.
38. Wu HM, Fornek M, Schwab KJ, Chapin AR, Gibson K, Schwab E, Spencer C, Henning K. A norovirus outbreak at a long-term-care facility: The role of environmental surface contamination. *Infect Control Hosp Epidemiol*. 2005; 26(10):802-810.
39. Nazaroff WW. Norovirus, gastroenteritis, and indoor environmental quality. *Indoor Air*. 2011;21(5):353-356.
40. Bonifait L, Charlebois R, Vimont A, Turgeon N, Veillette M, Longtin Y, Jean J, Duchaine C. Detection and quantification of airborne norovirus during outbreaks in healthcare facilities. *Clin Infect Dis*. 2015;61(3):299-304.
41. Marks PJ, Vipond IB, Carlisle D, Deakin D, Fey RE, Caul EO. Evidence for airborne transmission of Norwalk-like virus (NLV) in a hotel restaurant. *Epidemiol Infect*. 2000;124(3):481-487.

List of figures

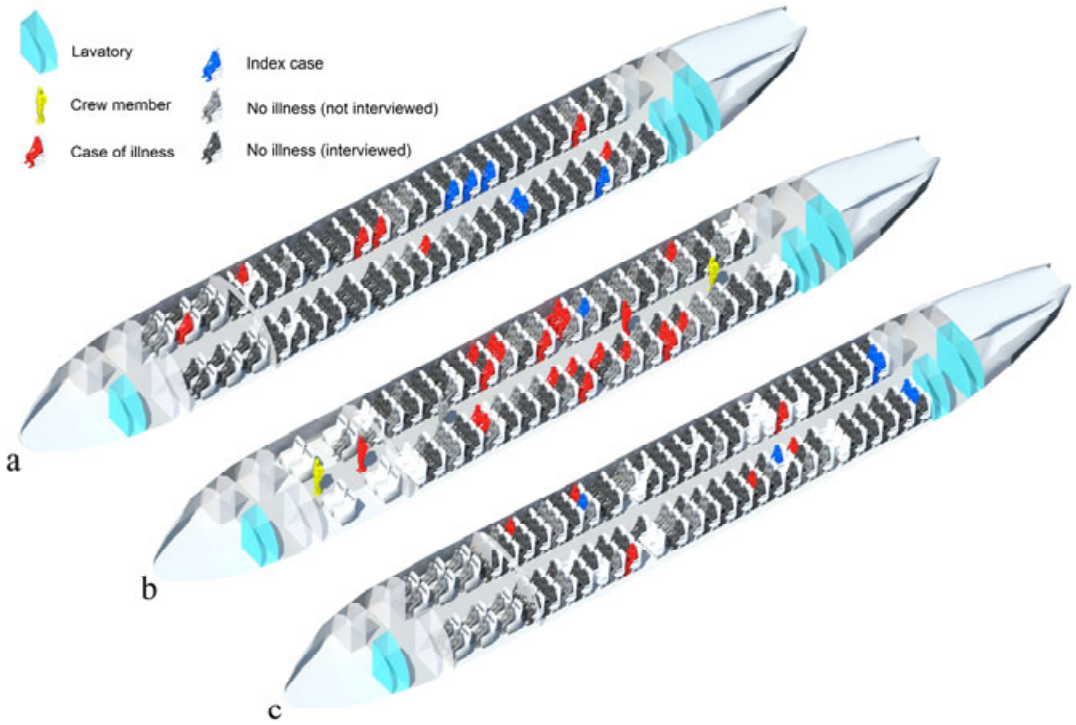

Figure 1 Spatial distribution for three inflight infection outbreaks, (a) norovirus,[26] (b) SARS CoV,[27] and (c) influenza A H1N1.[28]

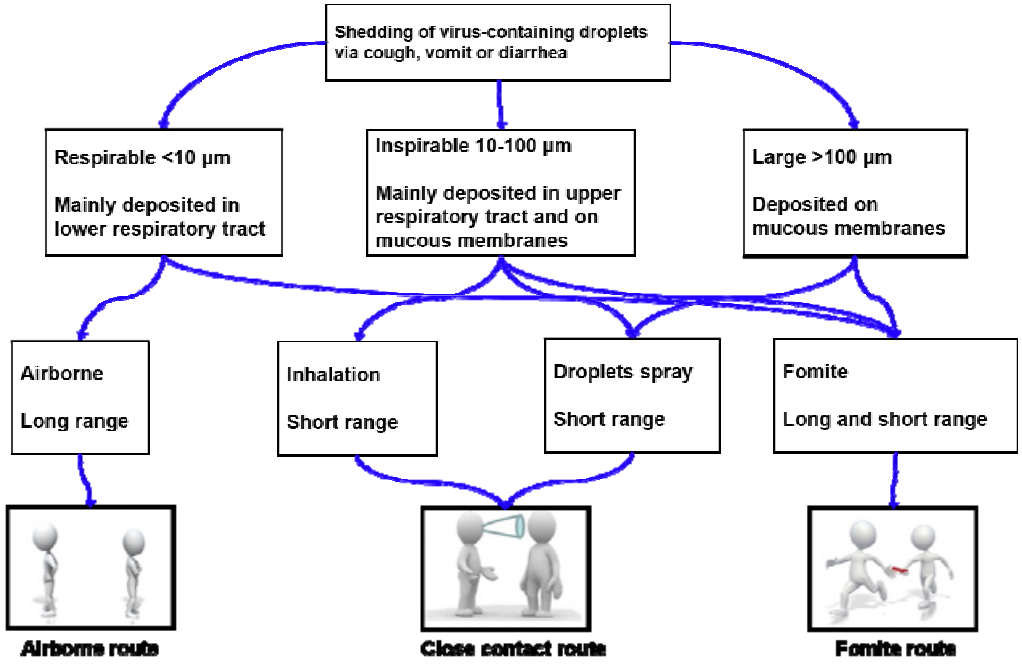

Figure 2 Illustration of different transmission routes considered in this study. Note that all sizes of droplets are involved in the fomite route.

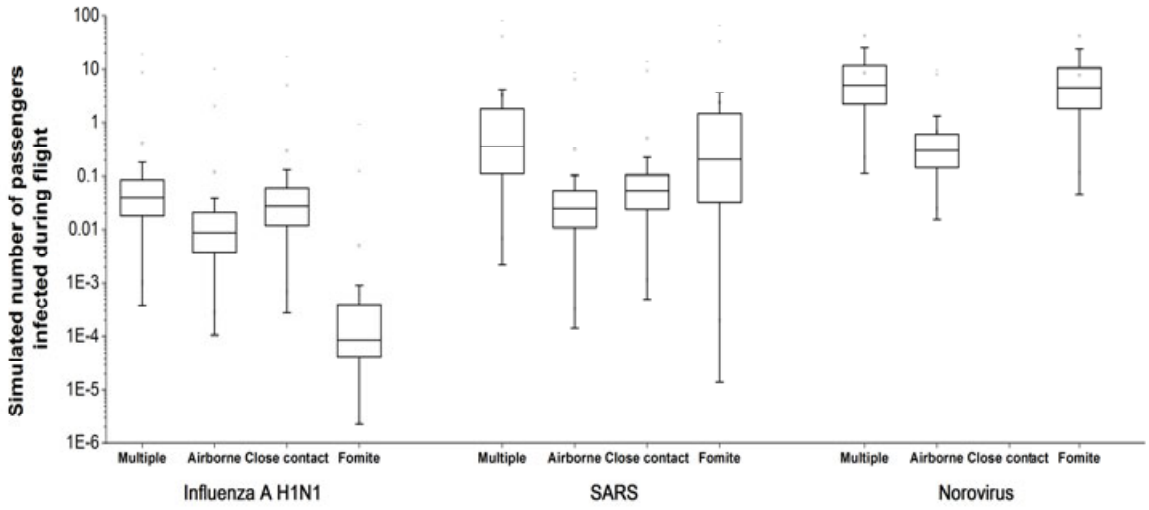

(a)

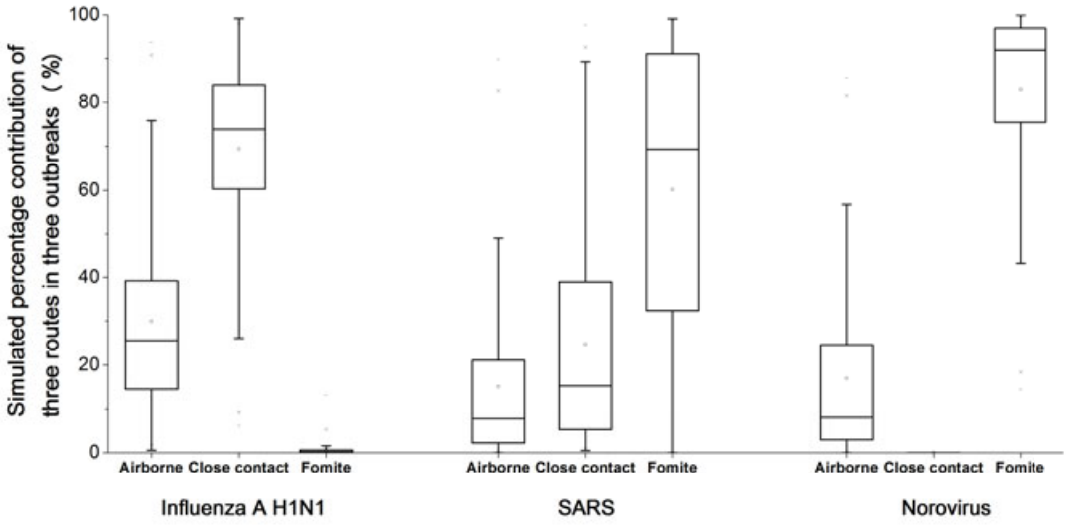

(b)

Figure 3. (a) Distribution of simulated number of passengers infected during flight and (b) percentage contribution of three transmission routes in three inflight outbreaks (with the full range of the virus shedding magnitudes). The box represents the interquartile range, and the horizontal line inside the box the median; vertical lines represent the maximum and minimum value without outliers.

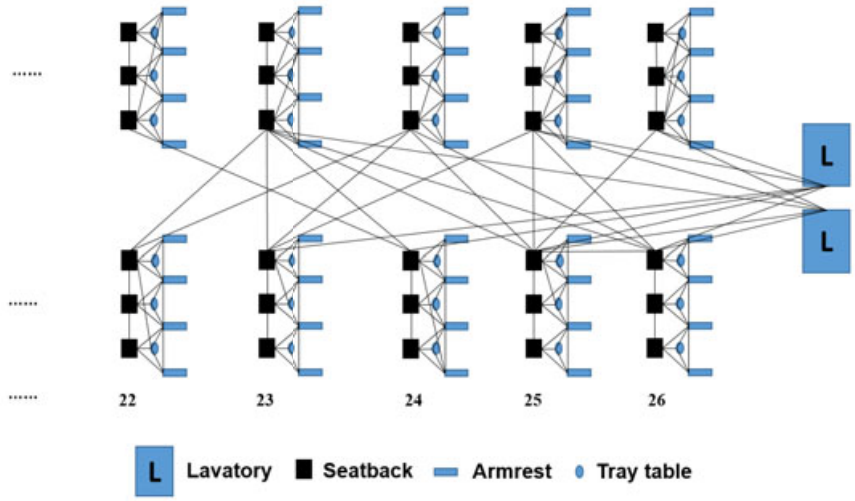

Figure 4 Part of the surface contamination network in one sample simulation.

List of tables

Table 1 Reported attack rate, predicted average infection risks and number of passengers infected by three transmission routes respectively (with the tuned range of the virus shedding magnitudes).

	Reported attack rate	Simulated average infection risk [95% CI]	Simulated average number of passengers infected via three routes respectively [95% CI]		
			Airborne	Close contact	Fomite
Influenza A H1N1	4.3% (4/93)	3.8% [3.5%, 4.2%]	1.9 [1.5, 2.2]	3.6 [3.2, 4.0]	0.04 [0.03, 0.05]
SARS CoV	16.4% (18/110)	19.8% [18.3%, 21.3%]	4.3 [3.6, 4.9]	4.8 [4.5, 5.1]	14.5 [13.1, 16.0]
Norovirus	8.6% (6/70)	9.4% [8.4%, 10.4%]	0.7 [0.5, 0.8]	0 [0, 0]	7.9 [7.0, 8.8]

Table 2 Infection risks of passengers within two rows of the index case(s) and others from the simulation results and reported outbreak data respectively (with the tuned range of the virus shedding magnitudes).

	Average infection risk		Statistical properties from outbreak data[a]
	Simulation results within two rows [95% CI] {others [95% CI]}	**Outbreak data** within two rows {others}	
Influenza A H1N1	14.0% [12.6%, 15.4%] {2.0% [1.7%, 2.3%]}	17.6% (3/17) {1.3% (1/76)}	*P*=0.019 RR:13.4 95% CI:1.5-121.2
SARS CoV[b]	41.2% [38.8%, 43.8%] {14.7% [13.3%, 16.0%]}	26.1% (6/23)[a] {13.8% (12/87)}	*P*=0.137 RR: 1.9 95% CI: 0.80-4.50
Norovirus	Not applicable	Not applicable	Not applicable

a 1-sided Chi-square test was used to test whether the passengers within two rows of the index case(s) had a statistically significant higher infection risk than others, the *P* value (Exact Significance. (1-side)), relative risk and 95% CI are quoted. The *P* value <0.05 was considered significant.

Table 3 Reported and simulated infection risk for aisle and non-aisle seat passengers respectively (with the tuned range of the virus shedding magnitudes).

	Average infection risk		Statistical properties from outbreak data[a]
	Simulation results Aisle seats [95% CI] {others [95% CI] }	**Outbreak data** Aisle seats {others}	
Influenza A H1N1	4.4% [4.0%, 4.9%] {3.6% [3.2%, 3.9%]}	6.1% (2/33) {3.3% (2/60)}	*P*=0.446 RR: 1.8 95% CI: 0.27-12.3
SARS CoV	26.1% [24.1%, 28.0%] {16.7% [15.4%, 17.9%]}	15.8% (6/38) {16.7% (12/72)}	*P*=0.568 RR: 0.95 95% CI: 0.39-2.33
Norovirus	14.7% [13.1 %, 16.3%] {7.0% [6.1%, 7.7%]}	20.8% (5/24) {2.2% (1/46)}	*P*=0.022 RR: 9.5 95% CI: 1.2-77.4

a 1-sided Chi-square test was used to test whether the aisle passengers had a statistically significant higher infection risk than others, the *P* value (Exact Significance. (1-side)), relative risk and 95% CI are quoted. The *P* value <0.05 was considered significant.